

# Synchronization of two different chaotic systems using novel adaptive interval type-2 fuzzy sliding mode control

Mehdi Roopaei · Mansoor Zolghadri Jahromi ·  
Bijan Ranjbar-Sahraei · Tsung-Chih Lin

Received: 22 October 2010 / Accepted: 28 December 2010 / Published online: 28 January 2011  
© Springer Science+Business Media B.V. 2011

**Abstract** In this paper, we use sliding mode control integrated with an interval type-2 fuzzy system for synchronization of two different chaotic systems in presence of system unmodeling and external disturbances. To reduce the chattering and improve the robustness of reaching phase of the Sliding Mode Control (SMC), an interval fuzzy type-2 logic controller is used. In addition, an adaptive interval type-2 fuzzy inference approximator is proposed (as equivalent control part of SMC) to approximate the unknown parts of the uncertain chaotic system. Using type-2 fuzzy systems makes more effective synchronization results in presence of system uncertainty and disturbances in comparison with type-1 fuzzy approximators. The stability analysis for the proposed control scheme is provided, and simulation results compare the performance of interval type-2 fuzzy and type-1 fuzzy con-

trollers to verify the effectiveness of the proposed method.

**Keywords** Synchronization · Chaotic systems · Interval type-2 fuzzy controller · Sliding mode control

## 1 Introduction

Since the publication of two relevant papers by Ott et al. [1] and Pecora et al. [2] in 1990, control and synchronization of chaos have become very important topics on the applications of nonlinear systems, and different approaches for chaos synchronization have been proposed by many researchers. Many applications of chaos synchronization in physical, chemical, biological, and many other practical systems are the reason for such an immense interest. Some possible application areas are in secure communications, optimization of nonlinear systems performance, modeling brain activity, and pattern recognition phenomena [1–6]. We also note that, in a wider sense, nonlinear dynamics can play an extremely important role in resolving outstanding problems in theoretical physics [7].

Synchronization of chaotic systems is a difficult task as the characteristic of chaos is extremely sensitivity to initial conditions. In 1993, the cascade synchronization method [8] was presented by Pecora and Carroll. They demonstrated that the cascading of synchronized chaotic systems allows the reproduction of

---

M. Roopaei (✉) · M. Zolghadri Jahromi ·  
B. Ranjbar-Sahraei  
School of Electrical and Computer Engineering, Shiraz  
University, Shiraz, Iran  
e-mail: mehdi.roopaei@gmail.com

M. Zolghadri Jahromi  
e-mail: zjahromi@shirazu.ac.ir

B. Ranjbar-Sahraei  
e-mail: b.ranjbar@ieee.org

T.-C. Lin  
Department of Electronic Engineering, Feng-Chia  
University, Taichung, Taiwan  
e-mail: tclin@fcu.edu.tw

all of the signals in the original chaotic system using only one signal to monitor the synchronized motions.

Recently, the study of chaos synchronization has become a hot spot in the nonlinear dynamics field, and researchers in this field have explored a variety of problems on chaos synchronization, such as the stability conditions for chaos synchronization, the realization for a successful synchronization, the applications of chaos synchronization, and so on [9–16].

In the past 15 years, many techniques for chaos control and synchronization have been developed. These include periodic parametric perturbation [17], drive-response synchronization [18], adaptive control [19–23], variable structure (or sliding mode) control [24–26], backstepping control [27, 28],  $H_\infty$  control [29], fuzzy control [30], and many others.

Since Zadeh [31] initiated the fuzzy set theory, Fuzzy Logic Control (FLC) schemes have been widely developed and successfully applied to many real-world applications [32]. Besides, adaptive FLC schemes have been used to control and synchronize the chaotic systems [33, 34]. In recent years it is shown that type-1 fuzzy systems have difficulties in modeling and minimizing the effect of rule and data uncertainties [35–41]. One reason is that a type-1 fuzzy set is certain in the sense that the membership grade for a particular input is a crisp value. The type-2 fuzzy sets which are characterized by membership functions (MF) that are themselves fuzzy was first introduced by Zadeh [42] and has been attracting many interests [35–41]. For such type-2 sets, each input has unity secondary membership grade defined by two type-1 MF, upper MF, and lower MF.

Recently, type-2 fuzzy sets have been successfully applied on different applications as type-2 fuzzy neural network [43], image processing [44], embedding intelligent agents [45], pattern recognition [46, 47], mobile robots control [48], and fuzzy controller designs [49, 50].

In this paper, the proposed Adaptive Interval type-2 Fuzzy Controller (AIT2FC) integrated with Sliding Mode Controller (SMC) methodology can synchronize two chaotic oscillators in the presence of data uncertainties, unpredicted internal disturbance, and external disturbances (in both of master and slave systems). To design the reaching phase of the SMC, a type-2 fuzzy logic controller is used. This will reduce the chattering and improves the robustness of the scheme. A type-2 fuzzy approximator is also used

as equivalent control part of SMC to approximate the unknown parts of the uncertain system using type-2 fuzzy sets.

One of the most important issues for fuzzy control systems is how to deal with the guarantee of stability and control performance. In this paper, we prove the closed-loop system global stability in the Lyapunov sense. Simulation results show that the AIT2FSMC can achieve a certain goal accurately in the presence of significant plant uncertainties without concern for external disturbances.

The rest of this paper is organized as follows: Sect. 2 presents system description. A brief description of interval type-2 fuzzy systems is introduced in Sect. 3. Design of the proposed controller is discussed in Sect. 4. Simulation results are given in Sect. 5. Finally, conclusions are given in Sect. 6.

## 2 System description and problem formulation

In this paper, we study a class of chaotic  $n$ -dimensional systems having the following system description:

Master System

$$\begin{cases} \dot{x}_i = x_{i+1}, & 1 \leq i \leq n-1 \\ \dot{x}_n = g(x, t) \end{cases}$$

$$x = [x_1, x_2, \dots, x_n] \in \mathbb{R}^n \quad (1)$$

Slave System

$$\begin{cases} \dot{y}_i = y_{i+1}, & 1 \leq i \leq n-1 \\ \dot{y}_n = f(y, t) + d(t) + u \end{cases}$$

$$y = [y_1, y_2, \dots, y_n] \in \mathbb{R}^n \quad (2)$$

where  $u \in \mathbb{R}$  is the control input,  $f$  and  $g$  are unknown nonlinear functions, and  $d(t)$  is the disturbance of system (2).

In general, the uncertainty and disturbance are assumed to be bounded as follows:

$$\begin{cases} |g(x, t)| \leq G < \infty \\ |f(y, t)| \leq F < \infty \\ |d(t)| \leq \beta \end{cases} \quad (3)$$

for all  $x \in U_x \subset \mathbb{R}^n$  and  $y \in U_y \subset \mathbb{R}^n$ , where  $U_x$  and  $U_y$  are compact sets defined as  $U_x = \{x \in \mathbb{R}^n : \|x\| \leq m_x < \infty\}$  and  $U_y = \{y \in \mathbb{R}^n : \|y\| \leq m_y < \infty\}$ ,

and  $G, F, \beta$  are known constants. System (1) is usually applied to physical systems such as the Duffing–Holmes damped spring system, the Van der Pol equation, Genesio system [51], robot systems, and flexible-joint mechanisms [52]. It is also assumed that  $f(y, t)$  and  $g(x, t)$  satisfy all the necessary conditions, such as systems (1) and (2) having unique solution in the time interval  $[t_0, +\infty], t_0 > 0$ , for any given initial condition  $x_0 = x(t_0)$  and  $y_0 = y(t_0)$ . In addition, without control input (i.e.,  $u(t) = 0$ ), system (1) displays chaotic motion.

Because of the butterfly effect, which causes the exponential divergence of the trajectories of two chaotic systems started with different initial conditions, having two chaotic systems evolving in synchrony might appear quite surprising. The control problem considered in this paper is that for different initial conditions of systems (1) and (2), the two coupled systems (i.e., the master system (1) and the slave system (2)) are to be synchronized by designing an appropriate control  $u(t)$  in system (2) such that

$$\lim_{t \rightarrow \infty} \|y(t) - x(t)\| \rightarrow 0 \tag{4}$$

where  $\|\cdot\|$  denotes the Euclidian norm of a vector.

Let us define state errors between the master and slave systems as

$$e_1 = y_1 - x_1, \quad e_2 = y_2 - x_2, \dots \tag{5}$$

$$e_n = y_n - x_n$$

$$\begin{cases} \dot{e}_1 = e_2 \\ \dot{e}_2 = e_3 \\ \vdots \\ \dot{e}_{n-1} = e_n \\ \dot{e}_n = f(y, t) - g(x, t) + d(t) + u(t) \end{cases} \tag{6}$$

The synchronization problem can be viewed as the problem of choosing an appropriate control law  $u(t)$  such that the error states  $e_i$  ( $i = 1, 2, \dots, n$ ) in (6) converge to zero.

### 3 Interval Type-2 Fuzzy Logic System

Fuzzy Logic Systems (FLSs) are known as the universal approximators and have various applications in identification and control design. A type-1 fuzzy system consists of four major parts: fuzzifier, rule base,

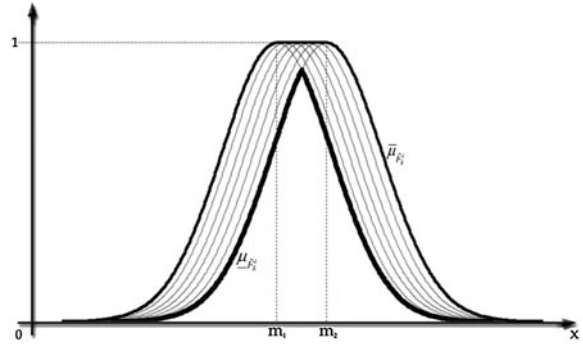


Fig. 1 Interval type-2 fuzzy set (IT2FS)

inference engine, and defuzzifier. A type-2 fuzzy system has a similar structure, but one of the major differences can be seen in the rule base part, where a type-2 rule base has antecedents and consequents using Type-2 Fuzzy Sets (T2FS). In a T2FS, a Gaussian function with a known standard deviation is chosen, while the mean ( $m$ ) varies between  $m_1$  and  $m_2$ . Therefore, a uniform weighting is assumed to represent a footprint of uncertainty as shaded in Fig. 1. Because of using such a uniform weighting, we name the T2FS as an Interval Type-2 Fuzzy Set (IT2FS).

Utilizing a rule base which consists of IT2FSs, the output of the inference engine will also be a T2FS, and therefore, we need a type-reducer to convert it to a type-1 fuzzy set before defuzzification can be carried out. Figure 2 shows the main structure of an interval type-2 FLS.

By using singleton fuzzification, the singleton inputs are fed into the inference engine. Combining the fuzzy if-then rules, the inference engine maps the singleton input  $x = [x_1, x_2, \dots, x_3]$  into a type-2 fuzzy set as the output. A typical form of an if-then rule is

$$R_i = \text{if } x_1 \text{ is } \tilde{F}_1^i \text{ and } x_2 \text{ is } \tilde{F}_2^i \text{ and } \dots \text{ and } x_n \text{ is } \tilde{F}_n^i \text{ then } \tilde{G}^i \tag{7}$$

where  $\tilde{F}_k^i$  s are the antecedents ( $k = 1, 2, \dots, n$ ), and  $\tilde{G}^i$  is the consequent of the  $i$ th rule. The sup-star method is chosen among various inference methods, and the first step to evaluate the firing set for  $i$ th rule is

$$F^i(x) = \prod_{k=1}^n \mu_{\tilde{F}_k^i}(x_k) \tag{8}$$

**Fig. 2** Main structure of an Interval Type-2 FLS (IT2FLS)

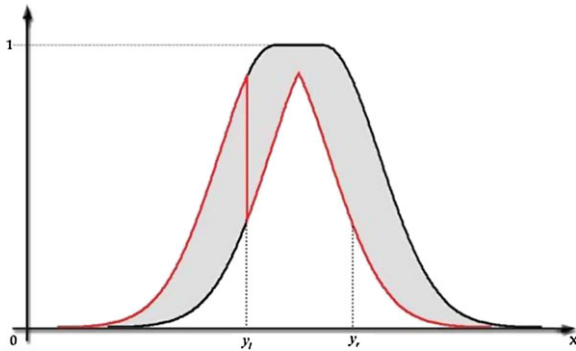
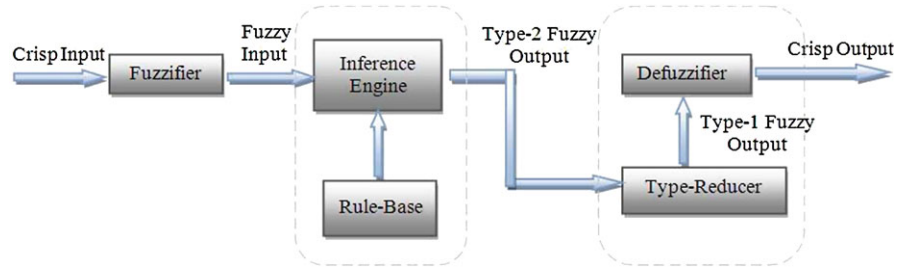


**Fig. 3** Computing right and left centroids for an IT2FS

As all of the  $\tilde{F}_k^i$ 's are IT2FSs, so  $F^i(\underline{x})$  can be written as  $F^i(\underline{x}) = [\underline{f}^i(\underline{x}) \ \bar{f}^i(\bar{x})]$ , where

$$\underline{f}^i(\underline{x}_i) = \prod_{k=1}^n \underline{\mu}_{\tilde{F}_k^i}(x_k) \tag{9}$$

$$\bar{f}^i(\underline{x}_i) = \prod_{k=1}^n \bar{\mu}_{\tilde{F}_k^i}(x_k) \tag{10}$$

The terms  $\underline{\mu}_{\tilde{F}_k^i}$  and  $\bar{\mu}_{\tilde{F}_k^i}$  are the lower and upper membership functions, respectively (Fig. 1).

In the next step, the firing set  $F^i(\underline{x})$  is combined with the  $i$ th consequent using the product t-norm to produce the type-2 output fuzzy set. The type-2 output fuzzy sets are then fed into the type reduction part. The structure of type reducing procedure is combined with the defuzzification procedure, which uses Center of Sets (COS) method. First, the left and right centroids of each rule consequent is computed using Karnik–Mendel (KM) algorithm [53] as shown in Fig. 3. Let us call it  $[y_l \ y_r]$ .

The firing sets  $F^i(\underline{x}) = [\underline{f}^i(\underline{x}) \ \bar{f}^i(\underline{x})]$  computed in inference engine are combined with the left and right centroids of consequents, and then the defuzzified output is evaluated by finding the solutions of the follow-

ing optimization problems:

$$y_l(\underline{x}) = \min_{\forall f^k \in \{\underline{f}^k \ \bar{f}^k\}} \left( \frac{\sum_{k=1}^M y_l^k f^k(\underline{x})}{\sum_{k=1}^M f^k(\underline{x})} \right) \tag{11}$$

$$y_r(\underline{x}) = \max_{\forall f^k \in \{\underline{f}^k \ \bar{f}^k\}} \left( \frac{\sum_{k=1}^M y_r^k f^k(\underline{x})}{\sum_{k=1}^M f^k(\underline{x})} \right) \tag{12}$$

Define  $f_l^k(\underline{x})$  and  $f_r^k(\underline{x})$  as the functions that are used to solve (11) and (12), respectively, and let  $\xi_l^k(\underline{x}) = f_l^k(\underline{x}) / \sum_{k=1}^M f_l^k(\underline{x})$  and  $\xi_r^k(\underline{x}) = f_r^k(\underline{x}) / \sum_{k=1}^M f_r^k(\underline{x})$ ; then (11) and (12) can be rewritten as

$$\begin{aligned} y_l(\underline{x}) &= \frac{\sum_{k=1}^M y_l^k f_l^k(\underline{x})}{\sum_{k=1}^M f_l^k(\underline{x})} = \sum_{k=1}^M y_l^k \xi_l^k(\underline{x}) \\ &= \theta_l^T \xi_l(\underline{x}) \end{aligned} \tag{13}$$

and

$$\begin{aligned} y_r(\underline{x}) &= \frac{\sum_{k=1}^M y_r^k f_r^k(\underline{x})}{\sum_{k=1}^M f_r^k(\underline{x})} = \sum_{k=1}^M y_r^k \xi_r^k(\underline{x}) \\ &= \theta_r^T \xi_r(\underline{x}) \end{aligned} \tag{14}$$

where

$$\xi_l(\underline{x}) = [\xi_l^1(\underline{x}) \ \xi_l^2(\underline{x}) \ \dots \ \xi_l^M(\underline{x})]$$

and

$$\xi_r(\underline{x}) = [\xi_r^1(\underline{x}) \ \xi_r^2(\underline{x}) \ \dots \ \xi_r^M(\underline{x})]$$

are the fuzzy basis functions, and

$$\theta_l(\underline{x}) = [y_l^1(\underline{x}) \ y_l^2(\underline{x}) \ \dots \ y_l^M(\underline{x})]$$

and

$$\theta_r(\underline{x}) = [y_r^1(\underline{x}) \ y_r^2(\underline{x}) \ \dots \ y_r^M(\underline{x})]$$

are the adjustable parameters.

Finally, the crisp value is obtained by the defuzzification procedure as

$$\begin{aligned} y(\underline{x}) &= \frac{1}{2} (y_l(\underline{x}) + y_r(\underline{x})) = \frac{1}{2} (\theta_l^T \xi_l(\underline{x}) + \theta_r^T \xi_r(\underline{x})) \\ &= \frac{1}{2} \theta^T \xi(\underline{x}) \end{aligned} \quad (15)$$

where  $\theta = [\theta_l^T \ \theta_r^T]^T$  and  $\xi = [\xi_l^T \ \xi_r^T]^T$ .

#### 4 Traditional SMC and controller design

SMC is an effective control methodology that has been successfully applied to the field of chaos synchronization.

SMC design generally consists of the following two main steps. Firstly, the selection of a sliding surface which induces a stable reduced-order dynamics assigned by the designer. Secondly, the synthesis of a switching control law to force the closed-loop system trajectory onto the sliding surface (and subsequently keeping it on that surface).

In traditional SMC, a sliding surface  $s$  representing the desired system dynamics is chosen as

$$s = e_n + \sum_{i=1}^{n-1} c_i e_i \quad (16)$$

The switching surface parameters  $\{c_i, i = 1, \dots, n - 1\}$  are chosen based on the following two criteria. First, the values are chosen to stabilize the system during the sliding mode. Routh–Hurwitz criterion [54] is used to determine the range of coefficients  $c_i$  that produce stable dynamics. That is, all the roots of the following characteristic polynomial describing the sliding surface have negative real parts with desirable pole placement.

$$P(\lambda) = \lambda^n + c_{n-1} \lambda^{n-1} + \dots + c_2 \lambda + c_1 \quad (17)$$

Second, the values are chosen such that the system during sliding mode has fast and smooth response.

When the closed loop system is in the sliding mode, it satisfies  $\dot{s} = 0$ , and then the equivalent control law is obtained by

$$u_{eq} = -f(y, t) + g(x, t) - d(t) - \sum_{i=1}^{n-1} c_i e_{i+1} \quad (18)$$

According to the Lyapunov stability theory [54], a Lyapunov function is defined as

$$V = \frac{1}{2} s^2 \quad (19)$$

Then, the derivative of  $V$  is

$$\dot{V} = s\dot{s} = s \left( \dot{e}_n + \sum_{i=1}^{n-1} c_i \dot{e}_i \right) \quad (20)$$

In the above equation, if  $\dot{V}$  is negative for all  $s \neq 0$ , then the so-called reaching condition [54] is satisfied. That is, the control signal  $u$  is designed to guarantee that the states are hitting on the sliding surface  $s = 0$ .

In the traditional SMC, the reaching control law is selected as  $u_r = k_w u_w$ , and the overall control  $u$  is determined by

$$u = u_{eq} + u_r = u_{eq} + k_w u_w \quad (21)$$

where,  $k_w$  is the switching gain, which is positive, and  $u_w$  is obtained by

$$u_w = \text{sgn}(s) \quad (22)$$

Based on Lyapunov theory, the system states approach the hyperplane if  $\dot{V} \leq -k_w |s|$ . The error vector asymptotically reduces to zero once the system states are on  $s = 0$ .

In our proposed controller, as  $f(y, t)$ ,  $g(x, t)$ , and  $d(t)$  are unknown terms in (18), the equivalent part is approximated by an Adaptive Interval Type-2 Fuzzy Inference Approximator (AIT2FIA). However, the sign function in reaching control (22) will cause the control input to produce chattering phenomenon. To overcome this problem, an Interval Type-2 Fuzzy Logic Controller (IT2FLC) is also applied to the system. In the following sections, each of the above components is described in detail.

##### 4.1 IT2FLC design for the reaching phase

The dynamic behavior of a type-2 fuzzy controller is characterized by a set of linguistic rules based on an expert's knowledge, which is somehow fuzzy. From this set of rules, the inference methodology of FLC will be able to provide appropriate control action.

We can determine  $u_w$  (22) by  $s$  in fuzzy sliding-mode control. The reaching law for our proposed control methodology is selected as

$$u_r = k_{fs} u_{fs} \quad (23)$$

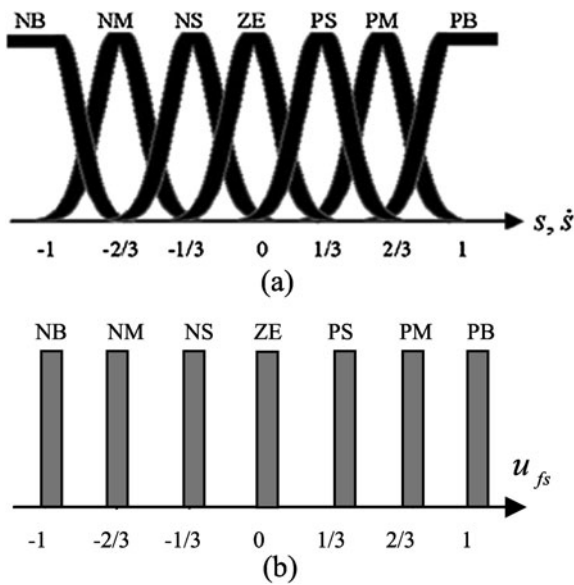


**Fig. 4** Fuzzy sets assigned to (a) input variables and (b) output variable

where  $k_{fs}$  is the normalization factor of the output variable, and  $u_{fs}$  is the output of the Fuzzy SMC (FSMC), which is determined by the normalized values of  $s$  and  $\hat{s}$ :

$$u_{fs} = FSMC(s, \hat{s}) \tag{24}$$

The type-2 membership functions used for the input variables  $s$  and  $\hat{s}$ , and output membership function  $u_{fs}$  are shown in Fig. 4. The fuzzy control rules provide the mapping of input linguistic variables to output linguistic variable  $u_{fs}$ . The fuzzy rule table was designed as in Table 1 [55].

4.2 AIT2FIA for the equivalent control part

Type-2 fuzzy systems are known as general function approximators. In AIT2FIA design, we use fuzzy systems to approximate the unknown functions  $f(y, t)$  and  $g(x, t)$ .

The input–output data points obtained from the systems construct the type-2 fuzzy models.

In order to use the equivalent control law given in (18), the functions  $f(y, t)$  and  $g(x, t)$  must be known, but in practice, these functions may be unknown for many real-life dynamical systems. To overcome this, we use Interval Type-2 Fuzzy Neural Network (IT2FNN) as shown in Fig. 5 to approximate the nonlinear functions  $f(y)$ ,  $g(x)$ . Then the adaptive

**Table 1** Rule-base of IT2FLC

|     |    | $\hat{s}$ |    |    |    |    |    |    |
|-----|----|-----------|----|----|----|----|----|----|
|     |    | PB        | PM | PS | ZE | NS | NM | NS |
| $s$ | PB | NB        | NB | NB | NB | NM | NS | ZE |
|     | PM | NB        | NB | NB | NM | NS | ZE | PS |
|     | PS | NB        | NB | NM | NS | ZE | PS | PM |
|     | ZE | NB        | NM | NS | ZE | PS | PM | PB |
|     | NS | NM        | NS | ZE | PS | PM | PB | PB |
|     | NM | NS        | ZE | PS | PM | PB | PB | PB |
|     | NB | ZE        | PS | PM | PB | PB | PB | PB |

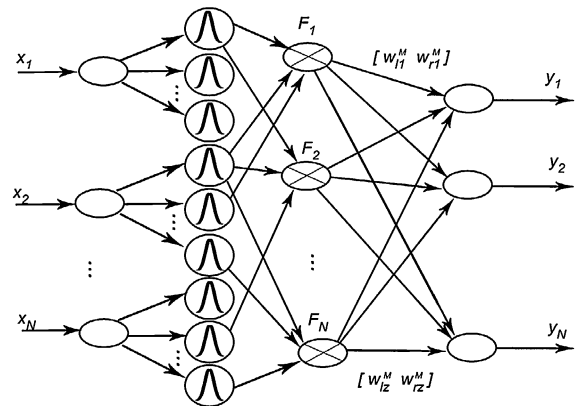


**Fig. 5** The structure of interval type-2 fuzzy neural network

laws will be developed for adjusting the parameters of IT2FNN to attenuate the approximation error and external disturbance.

Therefore, the nonlinear unknown functions  $f(y)$  and  $g(x)$  can be approximated by the fuzzy-neural approximators  $f(y|\theta_f)$  and  $g(x|\theta_g)$ , respectively:

$$f(y|\theta_f) = \frac{1}{2} [\xi_{fr}^T \ \xi_{fl}^T] \begin{bmatrix} \theta_{fr} \\ \theta_{fl} \end{bmatrix} = \theta_f^T \xi_f(y) \tag{25}$$

$$g(x|\theta_g) = \frac{1}{2} [\xi_{gr}^T \ \xi_{gl}^T] \begin{bmatrix} \theta_{gr} \\ \theta_{gl} \end{bmatrix} = \theta_g^T \xi_g(x) \tag{26}$$

where  $\theta_f$  and  $\theta_g$  are adjustable parameters vectors.

To derive the adaptive law for adjusting  $\theta_f$  and  $\theta_g$ , we first define the optimal parameter vector  $\theta_f^*$  and  $\theta_g^*$  as

$$\theta_f^* = \arg \min_{\theta_f \in \Omega_f} \left[ \sup_{y \in U_y} |f(y|\theta_f) - \hat{f}(y, t)| \right] \tag{27}$$

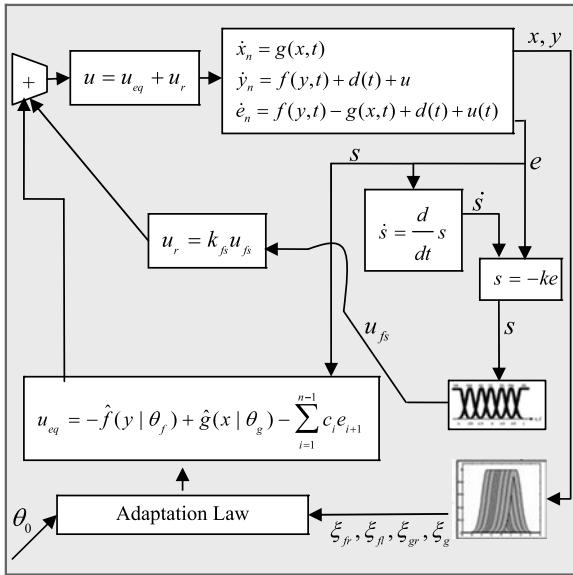


**Fig. 6** Overall scheme of the adaptive interval type-2 fuzzy control system

and

$$\theta_g^* = \arg \min_{\theta_g \in \Omega_g} \left[ \sup_{x \in U_X} |g(x|\theta_g) - \hat{g}(x, t)| \right] \quad (28)$$

where  $\theta_f$  and  $\theta_g$  belong to the compact sets  $\Omega_f$  and  $\Omega_g$ , respectively.

These sets are defined as  $\Omega_f = \{\theta_f \in \mathbb{R}^Q | \|\theta_f\| \leq m_f\}$  and  $\Omega_g = \{\theta_g \in \mathbb{R}^Q | \|\theta_g\| \leq m_g\}$ , where  $m_f$  and  $m_g$  are finite positive constants.

From (3), (27), and (28) we can conclude that  $|\hat{f}(y|\theta_f)| \leq F$  and  $|\hat{g}(x|\theta_g)| \leq G$ .

In practical systems, external disturbance  $d(t)$  is unknown. Thus, fuzzy models are used to construct the equivalent control law by replacing (18) with the following equation:

$$u_{eq} = -\hat{f}(y|\theta_f) + \hat{g}(x|\theta_g) - \sum_{i=1}^{n-1} c_i e_{i+1} \quad (29)$$

The overall control  $u$  is chosen as

$$u = u_{eq} + u_r = u_{eq} + k_{fs} u_{fs} \quad (30)$$

The block diagram of proposed adaptive interval type-2 fuzzy controller is shown in Fig. 6.

### 4.3 Stability analysis

In the following theorem, the proposed scheme will be proved to be able for deriving the nonlinear system (6)

onto the sliding mode ( $s = 0$ ). That is, the reaching condition  $s(t)\dot{s}(t) < 0$  is guaranteed.

Defining the minimum approximation error as

$$w = [f(y, t) - \hat{f}(y|\theta_f^*)] - [g(x, t) - \hat{g}(x|\theta_g^*)] \quad (31)$$

we can write

$$\begin{aligned} |w| &\leq |f(y, t) - \hat{f}(y|\theta_f^*)| + |g(x, t) - \hat{g}(x|\theta_g^*)| \\ &\leq \|\theta_f^{*T}\| \|\xi(y)\| + |f(y, t)| + \|\theta_g^{*T}\| \|\xi(x)\| \\ &\quad + |g(x, t)| \\ &\leq m_f + F + m_g + G \end{aligned} \quad (32)$$

and using equation  $m_f + F + m_g + G \leq \beta$ , it can be easily concluded that  $w$  is bounded, i.e.,

$$|w| \leq \beta \quad (33)$$

**Theorem 1** Consider that the uncertain nonlinear system (6) is controlled by  $u(t)$  in (30), where  $u_{eq}$  is (29),  $u_r$  is (23),  $u_{fs}$  is (24), and  $k_{fs} > \alpha + \beta$ . Then, the error state trajectory converges to the sliding surface  $s = 0$ .

*Proof of Theorem 1* In order to derive the adaptive law for adjusting  $\theta_{fl}$ ,  $\theta_{fr}$ ,  $\theta_{gl}$ , and  $\theta_{gr}$ , we consider the following Lyapunov function candidate:

$$\begin{aligned} V &= \frac{1}{2}s^2 + \frac{1}{4\gamma_{fl}} \Phi_{fl}^T \Phi_{fl} + \frac{1}{4\gamma_{fr}} \Phi_{fr}^T \Phi_{fr} \\ &\quad + \frac{1}{4\gamma_{gl}} \Phi_{gl}^T \Phi_{gl} + \frac{1}{4\gamma_{gr}} \Phi_{gr}^T \Phi_{gr} \end{aligned} \quad (34)$$

where  $\Phi_{fr} = \theta_{fr} - \theta_{fr}^*$ ,  $\dot{V} \leq -\eta|s|$ ,  $\Phi_{gr} = \theta_{gr} - \theta_{gr}^*$ ,  $\Phi_{gl} = \theta_{gl} - \theta_{gl}^*$ , and  $\gamma_{fr}$ ,  $\gamma_{fl}$ ,  $\gamma_{gr}$ , and  $\gamma_{gl}$  are arbitrary positive constants.

The time derivative of (34) is

$$\begin{aligned} \dot{V} &= s\dot{s} + \frac{1}{2\gamma_{fl}} \Phi_{fl}^T \dot{\Phi}_{fl} + \frac{1}{2\gamma_{fr}} \Phi_{fr}^T \dot{\Phi}_{fr} \\ &\quad + \frac{1}{2\gamma_{gl}} \Phi_{gl}^T \dot{\Phi}_{gl} + \frac{1}{2\gamma_{gr}} \Phi_{gr}^T \dot{\Phi}_{gr} \\ &= s \left[ \dot{e}_n + \sum_{i=1}^{n-1} c_i \dot{e}_i \right] + \frac{1}{2\gamma_{fl}} \Phi_{fl}^T \dot{\Phi}_{fl} + \frac{1}{2\gamma_{fr}} \Phi_{fr}^T \dot{\Phi}_{fr} \\ &\quad + \frac{1}{2\gamma_{gl}} \Phi_{gl}^T \dot{\Phi}_{gl} + \frac{1}{2\gamma_{gr}} \Phi_{gr}^T \dot{\Phi}_{gr} \\ &= \frac{1}{2}s \left[ f(y, t) - g(x, t) + d(t) + u + \sum_{i=1}^{n-1} c_i \dot{e}_i \right] \end{aligned}$$

$$\begin{aligned}
 & + \frac{1}{2\gamma_{fl}} \Phi_{fl}^T \dot{\Phi}_{fl} + \frac{1}{2\gamma_{fr}} \Phi_{fr}^T \dot{\Phi}_{fr} + \frac{1}{2\gamma_{gl}} \Phi_{gl}^T \dot{\Phi}_{gl} \\
 & + \frac{1}{2\gamma_{gr}} \Phi_{gr}^T \dot{\Phi}_{gr} \\
 = & \frac{1}{2} s [f(y, t) - \hat{f}(y|\theta_f^*) + \hat{f}(y|\theta_f^*) - \hat{f}(y|\theta_f) \\
 & - g(x, t) + \hat{g}(x|\theta_g^*) - \hat{g}(x|\theta_g^*) + \hat{g}(x|\theta_g) \\
 & + d(t)] + \frac{1}{2\gamma_{fl}} \Phi_{fl}^T \dot{\Phi}_{fl} + \frac{1}{2\gamma_{fr}} \Phi_{fr}^T \dot{\Phi}_{fr} \\
 & + \frac{1}{2\gamma_{gl}} \Phi_{gl}^T \dot{\Phi}_{gl} + \frac{1}{2\gamma_{gr}} \Phi_{gr}^T \dot{\Phi}_{gr} \\
 \leq & s w - s [\hat{f}(y|\theta_f) \hat{f}(y|\theta_f^*)] \\
 & + s [\hat{g}(x|\theta_g) - \hat{g}(x|\theta_g^*)] + \alpha |s| \\
 & - k_{fs} |s| + \frac{1}{2\gamma_{fl}} \Phi_{fl}^T \dot{\Phi}_{fl} + \frac{1}{2\gamma_{fr}} \Phi_{fr}^T \dot{\Phi}_{fr} \\
 & + \frac{1}{2\gamma_{gl}} \Phi_{gl}^T \dot{\Phi}_{gl} + \frac{1}{2\gamma_{gr}} \Phi_{gr}^T \dot{\Phi}_{gr} \\
 \leq & (\alpha + \beta - k_{fs}) |s| + \frac{1}{2} \Phi_{fr}^T \left( -s \xi_{fr}(y) + \frac{1}{\gamma_{fr}} \right) \\
 & + \frac{1}{2} \Phi_{fl}^T \left( -s \xi_{fl}(y) + \frac{1}{\gamma_{fl}} \right) \\
 & + \frac{1}{2} \Phi_{gr}^T \left( -s \xi_{gr}(x) + \frac{1}{\gamma_{gr}} \right) \\
 & + \frac{1}{2} \Phi_{gl}^T \left( -s \xi_{gl}(x) + \frac{1}{\gamma_{gl}} \right) \tag{35}
 \end{aligned}$$

Using the above equation, we choose the adaptive laws as

$$-s \xi_{fr}(y) + \frac{1}{\gamma_{fr}} \dot{\theta}_{fr} = 0 \Rightarrow \dot{\theta}_{fr} = \gamma_{fr} s \xi_{fr}(y) \tag{36}$$

$$-s \xi_{fl}(y) + \frac{1}{\gamma_{fl}} \dot{\theta}_{fl} = 0 \Rightarrow \dot{\theta}_{fl} = \gamma_{fl} s \xi_{fl}(y) \tag{37}$$

$$s \xi_{gr}(x) + \frac{1}{\gamma_{gr}} \dot{\theta}_{gr} = 0 \Rightarrow \dot{\theta}_{gr} = -\gamma_{gr} s \xi_{gr}(x) \tag{38}$$

$$s \xi_{gl}(x) + \frac{1}{\gamma_{gl}} \dot{\theta}_{gl} = 0 \Rightarrow \dot{\theta}_{gl} = -\gamma_{gl} s \xi_{gl}(x) \tag{39}$$

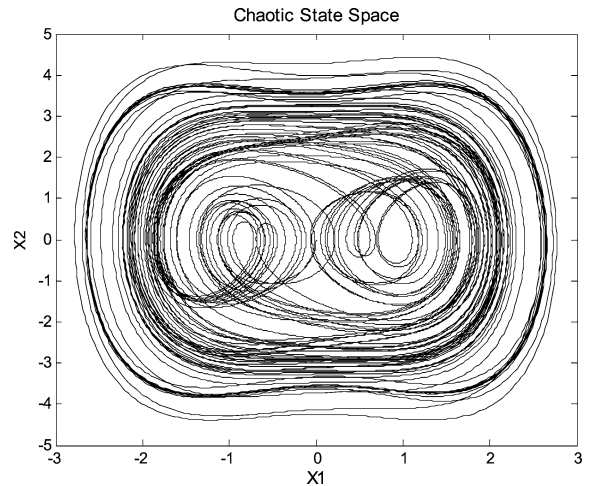


Fig. 7 Chaotic state space [57]

Therefore, we obtain

$$\dot{V} \leq -[k_{fs} - (\alpha + \beta)] |s| \tag{40}$$

By selecting  $k_{fs} - (\alpha + \beta) = \eta$  ( $k_{fs} > (\alpha + \beta)$ ) we have

$$\dot{V} \leq -\eta |s| \tag{41}$$

As a result, the system is stable, and the error will asymptotically converge to zero.  $\square$

### 5 Simulation result

In this section, a synchronization of two nonidentical chaotic systems is simulated. The simulation results of the proposed AIT2FSMC are compared with the traditional Adaptive Fuzzy SMC (AFSMC) [56].

The master system is described by the following differential equation [57]:

$$\begin{cases} \dot{x}_1 = x_2 \\ \dot{x}_2 = -0.4x_2 + 1.1x_1 - x_1^3 - 2.1 \cos(1.8t) \end{cases} \tag{42}$$

The chaotic behavior of this system is shown in Fig. 7.

The slave system is described by the following differential equation (Duffing System) [58]:

$$\begin{cases} \dot{y}_1 = y_2 \\ \dot{y}_2 = 1.8y_1 - 0.1y_2 - y_1^3 - 1.1 \cos(0.4t) \end{cases} \tag{43}$$

The above systems exhibit chaotic behavior as shown in Fig. 8.

The control objective is to synchronize the Duffing system with the master system. The control function  $u(t)$  is added into the slave system. System initial conditions are  $x(0) = [0, 0]^T$  and  $y(0) = [1, 1]^T$  for the master and slave systems, respectively, and the proposed control input signal, using (30), is described as

$$u = u_{eq} + u_r$$

$$= -\hat{f}(y|\theta_f) + \hat{g}(x|\theta_g) - \sum_{i=1}^{n-1} c_i e_{i+1} + k_{fs} u_{fs} \quad (44)$$

To design the equivalent part of control signal, the input variables of the fuzzy systems  $\hat{f}(y|\theta_f)$  and  $\hat{g}(x|\theta_g)$  are chosen as  $y = [y_1, y_2]$  and  $x = [x_1, x_2]$ . For each variable  $x_i, y_i, i = 1, 2$ , we define five type-2 Gaussian membership functions with initial values  $\theta_f(0) = O_{2 \times 5}$  and  $\theta_g(0) = O_{2 \times 5}$ . To design the reaching part of control signal, the input variables of the

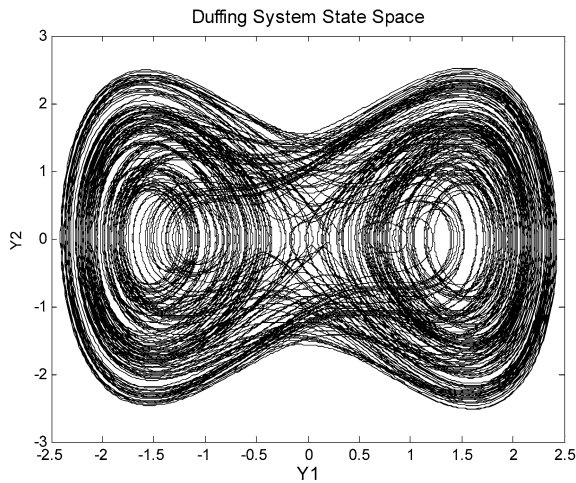
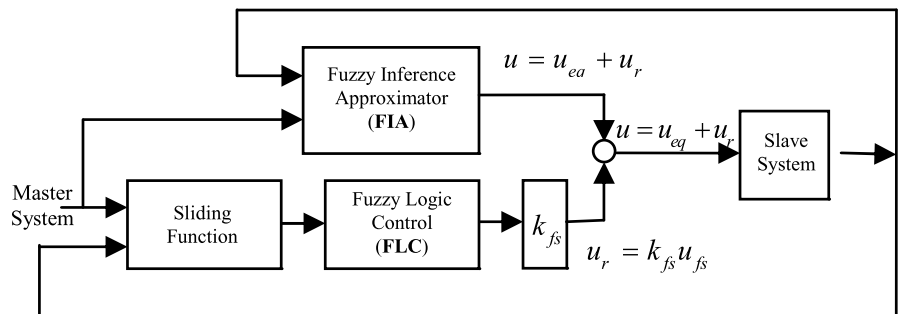


Fig. 8 Duffing system state space [58]

Fig. 9 Block diagram of adaptive interval type-2 fuzzy sliding mode controller



fuzzy system for  $u_{fs} = FSMC(s, \dot{s})$  are chosen as  $[s_n, \dot{s}_n]$ , where  $s_n = s/5$  and  $\dot{s}_n = \dot{s}/50$  are the normalized values of  $s$  and  $\dot{s}$ , then we define seven type-2 Gaussian membership functions as shown in Fig. 4(a).

The output singleton values for left mean and right mean are chosen as  $\theta_l = [-1.0, -0.7, -0.4, -0.1, 0.3, 0.6, 0.9]$  and  $\theta_r = [-0.9, -0.6, -0.3, 0.1, 0.4, 0.7, 1.0]$ , respectively (Fig. 4(b)), finally the design parameter used in (23) is chosen as  $k_{fs} = 5$ .

To illustrate the results, the performance of the proposed approach is evaluated for two experiments. In the first experiment, we give the simulation results of our proposed AIT2FSMC compared to traditional AFSMC [56] in synchronization of two aforementioned nonidentical chaotic systems. In the second experiment, the performance of the proposed controller is investigated in the presence of 20-Db noise applied to the measured states of both master and slave systems, while other conditions are the same as first experiment.

Experiment 1: Synchronization in the absence of noise

Two adaptive fuzzy controllers are considered with a common control structure as shown in Fig. 9. Simulation results using AIT2FSMC are compared with AFSMC [56].

State space trajectories and control input signals are illustrated in Figs. 10–11. In addition, to make the comparison between two methods more obvious, we focus on the first 0.4 seconds of the experiment time interval in Fig. 12.

Experiment 2: Synchronization in the presence of 20-Db noise

System synchronization in presence of 20-Db noise as shown in Fig. 13 is illustrated in this section, and

**Fig. 10** Synchronization using AFSMC [56] and AIT2FSMC

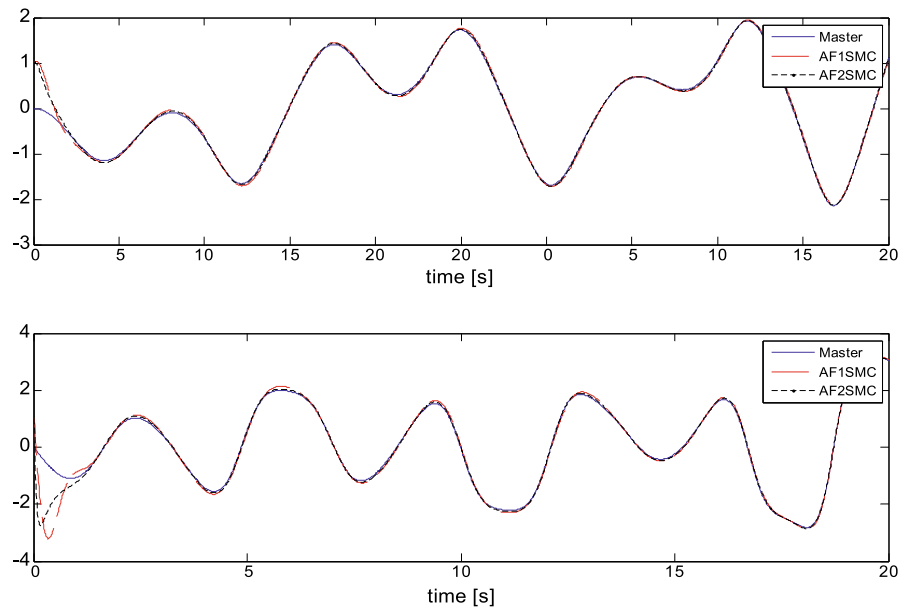


**Fig. 11** Control input for AFSMC [56] and AIT2FSMC

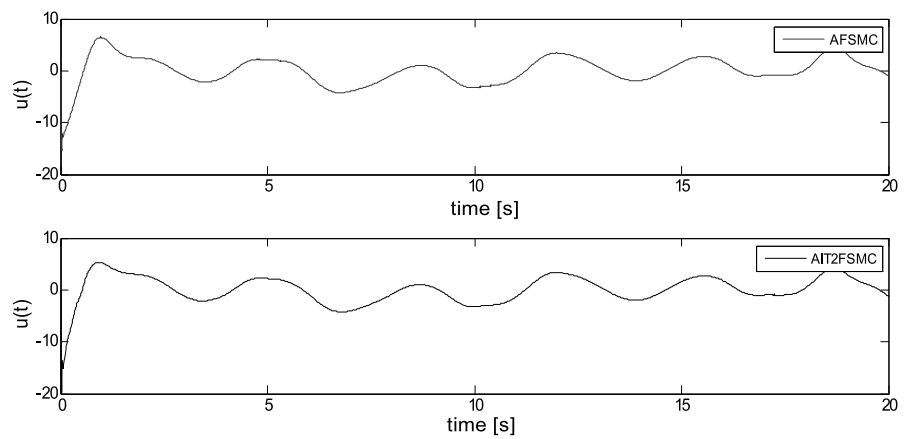


**Fig. 12** Synchronization of two chaotic systems using AFSMC [56] and AIT2FSMC in the interval of  $t = [0, 0.4]$  (the state  $y_1$  following  $x_1$  and the output of the slave  $y_2$  following the output of master the  $x_2$ )

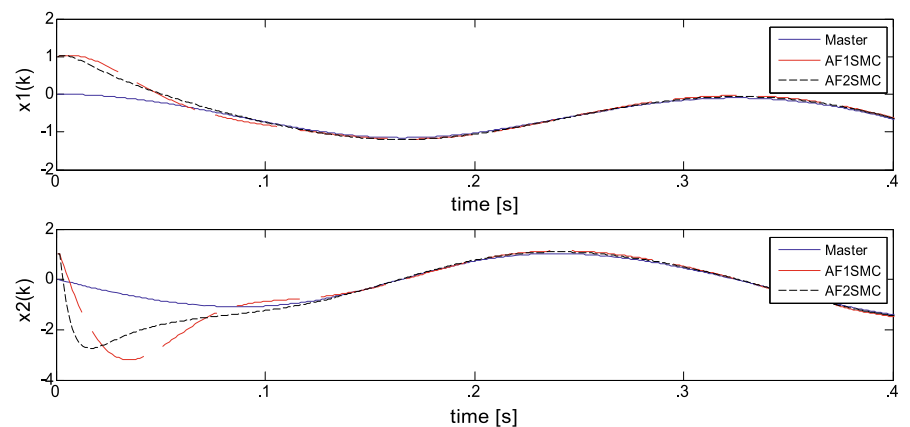


**Fig. 13** Block diagram of adaptive fuzzy sliding mode controller in presence of noise

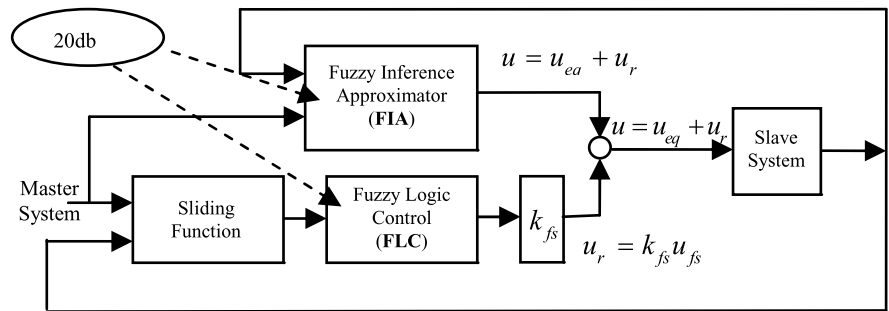


**Fig. 14** Synchronization of two chaotic systems using AFSMC [56] and AIT2FSMC in presence of 20-Db noise (the state  $y_1$  following  $x_1$  and the output of the slave  $y_2$  following the output of the master  $x_2$ )

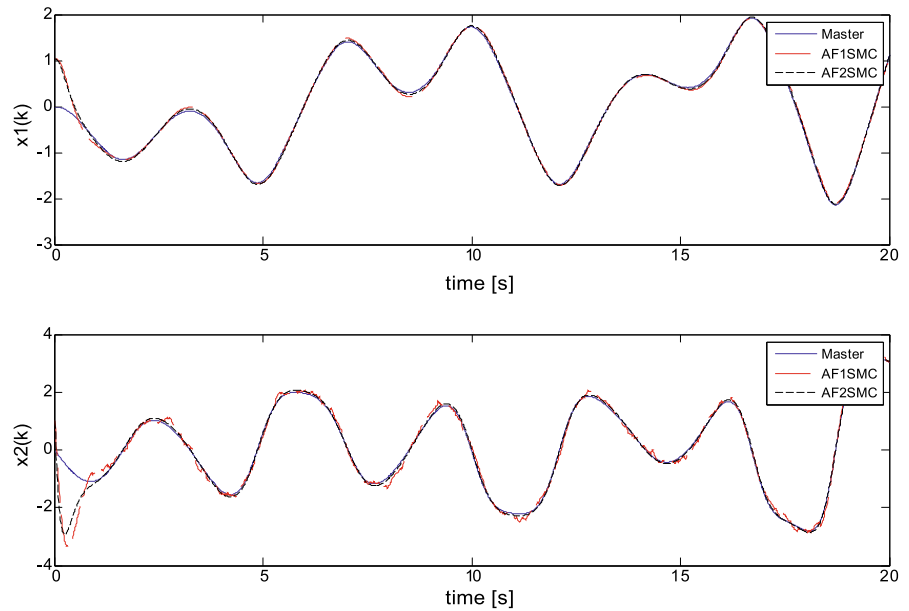
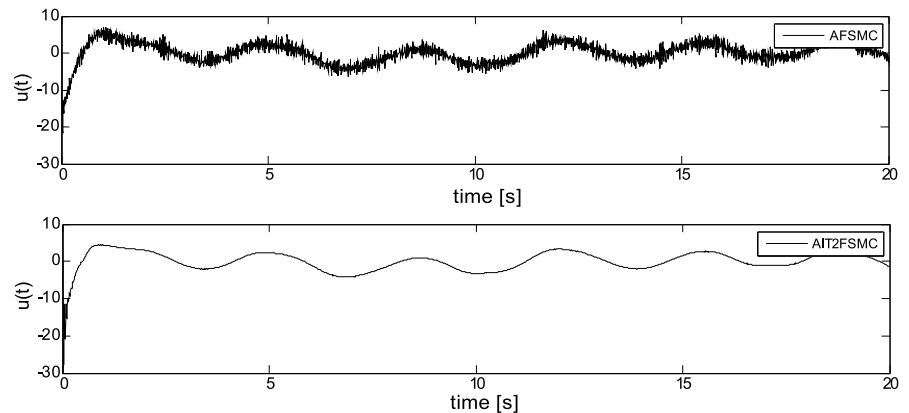


**Fig. 15** Control input for AFSMC [56] and AIT2FSMC in presence of 20-Db noise



AIT2F SMC and AFSMC [56] are compared. State space trajectories and control inputs are illustrated in Figs. 14–15.

The comparison between two methods can be more obvious when we focus on the first 0.4 seconds of the experiment time interval (Fig. 16). As can be seen,

**Table 2** IAE comparison between AIT2FSMC and AFSMC [56]

|                           |         | SNR = 20 | SNR = 26 | SNR = 38 | SNR = 44 | SNR = 50 |
|---------------------------|---------|----------|----------|----------|----------|----------|
| $\int_0^{20}  e_1(t)  dt$ | Type I  | 1.71     | 1.21     | 0.87     | 0.86     | 0.85     |
|                           | Type II | 1.28     | 0.98     | 0.81     | 0.80     | 0.79     |
| $\int_0^{20}  e_2(t)  dt$ | Type I  | 3.10     | 2.40     | 1.96     | 1.89     | 1.88     |
|                           | Type II | 2.43     | 2.06     | 1.87     | 1.86     | 1.85     |

**Fig. 16** Synchronization of two chaotic systems using AFSMC [56] and AIT2FSMC in presence of 20-Db noise in the interval of  $t = [0, 0.4]$  (the state  $y_1$  following  $x_1$  and the output of the slave  $y_2$  following the output of the master  $x_2$ )

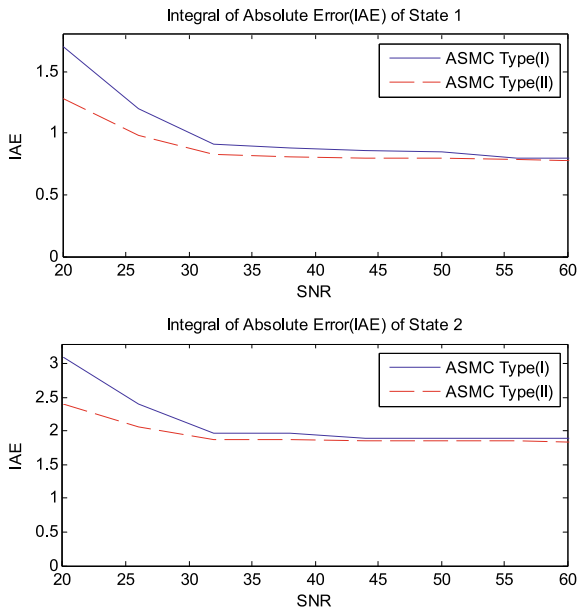
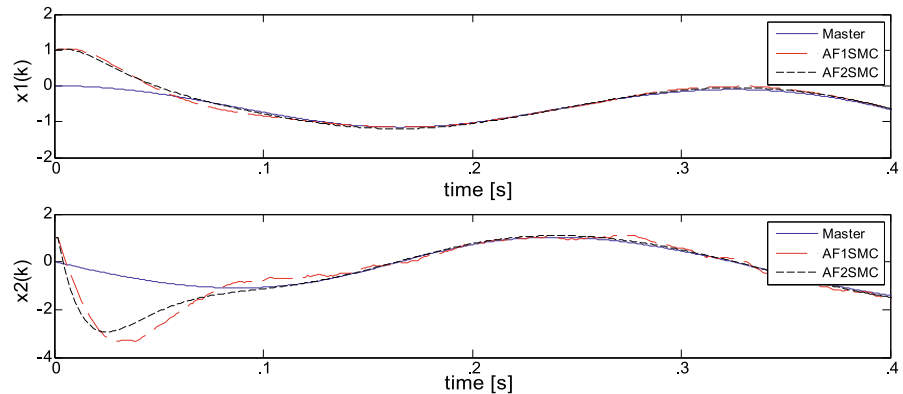


**Fig. 17** IAE of AFSMC [56] and AIT2FSMC when a white Gaussian noise is applied to the system

the synchronization performance of the interval type-2 fuzzy controller is better than the other one.

In order to have a quantitative comparison between different methods a white Gaussian noise is applied to the measured signal with various Signal

to Noise Ratios (SNRs). Integral of Absolute Error (IAE) is selected as the criterion. It is indicated that IAE for AIT2FSMC is much less than traditional AFSMC [56] in low SNRs, which shows the effectiveness of AIT2FSMC in the presence of noise (Fig. 17, Table 2).

The results in Table 2 clearly indicate that the performance of our proposed type-2 controller is better than type-1 method. As can be seen in high SNRs both of the methods have near performances but in low SNRs type-1 controller [56] has large IAEs while our proposed controller has still low IAEs.

### 6 Conclusion

In this paper, the synchronization problem for a class of uncertain chaotic systems in presence of external disturbance and internal uncertainties was investigated. Based on the Lyapunov stability theory, an Adaptive Interval Type-2 Fuzzy Sliding Mode Controller (AIT2FSMC) with corresponding parameter update laws was developed for global synchronization of the identical or nonidentical chaotic systems, where the structure of the controlled system is partially unknown. In addition, the major drawback of an SMC controller in a practical application, which is the chattering problem, is reduced by replacing the

relay control by an Interval Type-2 Fuzzy Logic Controller (IT2FLC). All the theoretical results are verified by numerical simulations to demonstrate the effectiveness of the proposed synchronization scheme.

## References

- Ott, E., Grebogi, C., Yorke, J.A.: Controlling chaos. *Phys. Rev. Lett.* **64**(11), 1196–1199 (1990)
- Pecora, L.M., Carroll, T.L.: Synchronization in chaotic systems. *Phys. Rev. Lett.* **64**(8), 821–824 (1990)
- Boccaletti, S., Kurthsv, J., Osiper, G.: The synchronization of chaotic systems. *Phys. Rep.* **366**, 1–101 (2002)
- Chen, G., Dong, X.: *From Chaos to Order Methodologies, Perspectives and Applications*. Singapore, World Scientific (1998)
- Schuster, H.G.: *Handbook of Chaos Control*. Wiley-VCH, New York-Weinheim (1999)
- Sprott, J.C.: *Chaos and Time-Series Analysis*. Oxford University Press, London (2003)
- Naschie, M.E.: Transfinite physics treading the path of Cantor and Einstein. *Chaos Solitons Fractals* **25**(4), 765–933 (2005)
- Carroll, T., Pecora, L.: Cascading synchronized chaotic. *Physica D* **67**, 126–140 (1993)
- Zhan, M., Hu, G., Yang, J.Z.: Synchronization of chaos in coupled systems. *Phys. Rev.* **62**, 2963–2966 (2002)
- Wang, S.H., Xiao, J.H., Wang, X.G., Hu, B., Hu, G.: Spatial orders appearing at instabilities of synchronous chaos of spatiotemporal systems. *Eur. Phys. J. B* **30**, 571–575 (2002)
- Guan, S.G., Lai, C.-H., Wei, G.W.: Bistable chaos without symmetry in generalized synchronization. *Phys. Rev.* **71**, 036209 (2005)
- Pisarchik, A.N., Pisarchik, A.N., Jaimes-Reátegui, R., Villalobos-Salazar, J.R., García-López, J.H., Boccaletti, S.: Synchronization of chaotic systems with coexisting attractors. *Phys. Rev. Lett.* **96**, 244102 (2006)
- Lai, Y.-C., Andrade, V.: Catastrophic bifurcation from riddled to fractal basins. *Phys. Rev. E* **64**, 056228 (2001)
- Barahona, M., Pecora, L.M.: Synchronization in Small-World Systems. *Phys. Rev. Lett.* **89**, 054101 (2002)
- Zhou, C.S., Kurths, J.: Dynamical weights and enhanced synchronization in adaptive complex networks. *Phys. Rev. Lett.* **96**, 164102 (2006)
- Zhou, C.S., Motter, A.E., Kurths, J.: Universality in the synchronization of weighted random networks. *Phys. Rev. Lett.* **96**, 034101 (2006)
- Astakhov, V.V., Anishchenko, V.S., Kapitaniak, T., Shabunin, A.V.: Synchronization of chaotic oscillators by periodic parametric perturbations. *Physica D* **109**, 11–16 (1997)
- Yang, X.S., Duan, C.K., Liao, X.X.: A note on mathematical aspects of drive-response type synchronization. *Chaos Solitons Fractals* **10**, 1457–1462 (1999)
- Wang, Y., Guan, Z.H., Wen, X.: Adaptive synchronization for Chen chaotic system with fully unknown parameters. *Chaos Solitons Fractals* **19**, 899–903 (2004)
- Chua, L.O., Yang, T., Zhong, G.Q., Wu, C.W.: Adaptive synchronization of Chua's oscillators. *Int. J. Bifurc. Chaos* **6**, 189–201 (1996)
- Liao, T.L.: Adaptive synchronization of two Lorenz systems. *Chaos Solitons Fractals* **9**, 1555–1561 (1998)
- Lian, K.Y., Liu, P., Chiang, T.-S., Chiu, C.-S.: Adaptive synchronization design for chaotic systems via a scalar driving signal. *IEEE Trans. Circuits Syst.* **49**, 17–27 (2002)
- Wu, C.W., Yang, T., Chua, L.O.: On adaptive synchronization and control of nonlinear dynamical systems. *Int. J. Bifurc. Chaos* **6**, 455–471 (1996)
- Fang, J.Q., Hong, Y., Chen, G.: Switching manifold approach to chaos synchronization. *Phys. Rev.* **59**, 2523–2526 (1999)
- Yin, X., Ren, Y., Shan, X.: Synchronization of discrete spatiotemporal chaos by using variable structure control. *Chaos Solitons Fractals* **14**, 1077–1082 (2002)
- Yu, X., Song, Y.: Chaos synchronization via controlling partial state of chaotic systems. *Int. J. Bifurc. Chaos* **11**, 1737–1741 (2001)
- Lu, J., Zhang, S.: Controlling Chen's chaotic attractor using backstepping design based on parameters identification. *Phys. Lett.* **286**, 145–149 (2001)
- Wang, C., Ge, S.S.: Adaptive synchronization of uncertain chaotic systems via backstepping design. *Chaos Solitons Fractals* **12**, 196–206 (2001)
- Suykens, J.A.K., Curran, P.F., Vandewalle, J., Chua, L.O.: Robust nonlinear  $H_\infty$  synchronization of chaotic Lur'e systems. *IEEE Trans. Circuits Syst.* **44**, 891–904 (1997)
- Tanaka, K., Ikeda, T., Wang, H.O.: A unified approach to controlling chaos via LMI-based fuzzy control system design. *IEEE Trans. Circuits Syst.* **45**, 1021–1040 (1998)
- Zadeh, L.A.: Fuzzy sets. *Inf. Control* **8**(3), 338–353 (1965)
- Kuo, C.L., Li, T.H., Guo, N.: Design of a novel fuzzy sliding-mode control for magnetic ball levitation system. *Journal of Intelligent and Robotic Systems* 1–22 (2004)
- Feng, G., Chen, G.: Adaptive control of discrete-time chaotic systems: a fuzzy control approach. *Chaos Solitons Fractals* **23**, 459–467 (2005)
- Xue, Y.J., Yang, S.Y.: Synchronization of generalized Henon map by using adaptive fuzzy controller. *Chaos Solitons Fractals* **17**, 717–722 (2003)
- Mendel, J.M.: Computing derivatives in interval type-2 fuzzy logic systems. *IEEE Trans. Fuzzy Syst.* **12**(1), 84–98 (2004)
- Wang, J.S., Lee, C.S.G.: Self-adaptive neuro-fuzzy inference systems for classification application. *IEEE Trans. Fuzzy Syst.* **10**(6), 790–802 (2002)
- Kovacic, Z., Balenovic, M., Bogdan, S.: Sensitivity based self learning fuzzy logic control for a servo system. *IEEE Control Syst. Mag.* **18**(3), 41–51 (1998)
- Golea, N., Golea, A., Benmahammed, K.: Fuzzy model reference adaptive control. *Fuzzy Sets and Systems* **137**(3), 353–366 (2003)
- Hojati, M., Gazor, S.: Hybrid adaptive fuzzy identification and control of nonlinear systems. *IEEE Trans. Fuzzy Syst.* **10**(2), 198–210 (2002)
- Lee, H., Tomizuka, M.: Robust adaptive control using a universal approximator for SISO nonlinear systems. *IEEE Trans. Fuzzy Syst.* **8**, 95–106 (2001)

41. Wang, C.H., Lee, C.S.: Dynamical optimal training for interval type-2 fuzzy neural network (T2FNN) Part B. *IEEE Trans. Syst. Man Cybern.* **34**(3), 1462–1477 (2004)
42. Zadeh, L.A.: The concept of a linguistic variable and its application to approximate reasoning-I. *Inf. Sci.* **8**, 199–249 (1975)
43. Zarandi, M.H.F., Burhan Türksen, I., Sobhani, J., Ramezani-pour, A.A.: Fuzzy polynomial neural networks for approximation of the compressive strength of concrete. *Appl. Soft. Comput.* **8**(1), 488–498 (2008)
44. Mendoza, O., Melin, P., Licea, G.: A hybrid approach for image recognition combining type-2 fuzzy logic, modular neural networks and the Sugeno integral. *Inf. Sci.* **179**(13), 2078–2101 (2009)
45. Doctor, F., Hagrass, H., Callaghan, V.: A type-2 fuzzy embedded agent to realise ambient intelligence in ubiquitous computing environments. *Inf. Sci.* **171**(4), 309–334 (2005)
46. Mitchell, H.B.: Pattern recognition using type-II fuzzy sets. *Inf. Sci.* **170**(2–4), 409–418 (2005)
47. Choi, B.I., Rhee, F.C.H.: Interval type-2 fuzzy membership function generation methods for pattern recognition. *Inf. Sci.* **179**(13), 2102–2122 (2009)
48. Martínez, R., Castillo, O., Aguilar, L.T.: Optimization of interval type-2 fuzzy logic controllers for a perturbed autonomous wheeled mobile robot using genetic algorithms. *Inf. Sci.* **179**(13), 2158–2174 (2009)
49. Jamaludin, J., Rahim, N.A., Hew, W.P.: Development of a self-tuning fuzzy logic controller for intelligent control of elevator systems. *Eng. Appl. Artif. Intell.* **22**(8), 1167–1178 (2009)
50. Lin, T.C., Liu, H.L., Kuo, M.J.: Direct adaptive interval type-2 fuzzy control of multivariable nonlinear systems. *Eng. Appl. Artif. Intell.* **22**(3), 420–430 (2009)
51. Park, J.H.: Synchronization of Genesio chaotic system via backstepping approach. *Chaos Solitons Fractals* **27**, 369–375 (2006)
52. Slotine, E., Li, W.: *Applied Nonlinear Control*. Englewood Cliffs, Prentice-Hall (1991)
53. Mendel, J.M.: Computing derivatives in interval type-2 fuzzy logic systems. *IEEE Trans. Fuzzy Syst.* **12**(1), 84–98 (2004)
54. Edwards, C., Spurgeon, S.K.: *Sliding Mode Control: Theory and Applications*. CRC Press, Boca Raton (1998)
55. Yau, T., Chen, C.L.: Chattering-free fuzzy sliding-mode control strategy for uncertain chaotic systems. *Chaos Solitons Fractals* **30**, 709 (2006)
56. Roopaei, M., Zolghadri Jahromi, M.: Synchronization of two different chaotic systems using novel adaptive fuzzy sliding mode control. *Chaos* **18**, 033133 (2008)
57. Wang, B., Wen, G.: On the synchronization of a class of chaotic systems based on backstepping method. *Phys. Lett. A* **370**(1), 35–39 (2007)
58. Liu, B., Zhou, Y., Jiang, M., Zhang, Z.: Synchronizing chaotic systems using control based on tridiagonal structure. *Chaos Solitons Fractals* **39**(5), 2274–2281 (2009)